

The Presence of the pAA Plasmid in the German O104:H4 Shiga Toxin Type 2a (Stx2a)–Producing Enteroaggregative *Escherichia coli* Strain Promotes the Translocation of Stx2a Across an Epithelial Cell Monolayer

Nadia Boisen,¹ Anne-Marie Hansen,² Angela R. Melton-Celsa,³ Tonia Zangari,³ Ninell Pollas Mortensen,^{4,5} James B. Kaper,² Alison D. O'Brien,³ and James P. Nataro¹

¹Department of Pediatrics, University of Virginia School of Medicine, Charlottesville; ²Department of Microbiology and Immunology, University of Maryland School of Medicine, Baltimore, and ³Department of Microbiology and Immunology, Uniformed Services University of the Health Sciences, Bethesda, Maryland; ⁴Technology for Industry and the Environment, Discovery–Science–Technology, RTI International, Research Triangle Park, North Carolina; and ⁵Biological and Nanoscale Systems, BioSciences Division, Oak Ridge National Laboratory, Tennessee

(See the editorial commentary by Steiner on pages 1860–2.)

Background. A Shiga toxin type 2a (Stx2a)–producing enteroaggregative *Escherichia coli* (EAEC) strain of serotype O104:H4 caused a large outbreak in 2011 in northern Europe. Pathogenic mechanisms for this strain are unclear. We hypothesized that EAEC genes encoded on the pAA virulence plasmid promoted the translocation of Stx2a across the intestinal mucosa.

Methods. We investigated the potential contribution of pAA by using mutants of Stx-EAEC strain C227-11, either cured of the pAA plasmid or deleted for individual known pAA-encoded virulence genes (ie, *aggR*, *aggA*, and *sepA*). The resulting mutants were tested for their ability to induce interleukin 8 (IL-8) secretion and translocation of Stx2a across a polarized colonic epithelial (T84 cell) monolayer.

Results. We found that deletion of *aggR* or *aggA* significantly reduced bacterial adherence and (independently) translocation of Stx2a across the T84-cell monolayer. Moreover, deletion of *aggR*, *aggA*, *sepA*, or the Stx2a-encoding phage from C227-11 resulted in reduced secretion of IL-8 from the infected monolayer.

Conclusions. Our data suggest that the AggR-regulated aggregative adherence fimbriae I enhance inflammation and enable the outbreak strain to both adhere to epithelial cells and translocate Stx2a across the intestinal epithelium.

Keywords. enteroaggregative *Escherichia coli* (EAEC); O104:H4; Shiga toxin; pAA plasmid; diarrhea.

Enteroaggregative *Escherichia coli* (EAEC) is a pathotype of diarrheagenic *Escherichia coli* that is a cause of acute and persistent diarrhea in many settings [1–7]. EAEC strains express a heterogeneous array of putative virulence factors [8–12] encoded on the bacterial chromosome or on the EAEC-specific pAA plasmid. EAEC

strains often harbor a transcriptional activator of the AraC/XylS class, called “AggR” [13], which controls genes on both the plasmid and the chromosome. Among the genes under AggR control include those that encode the aggregative adherence fimbriae (AAF), of which at least 4 variants exist [14–18]. AAF adhesins have been shown to be essential for EAEC adherence to human intestinal explants and to elicit both cytokine release and opening of epithelial tight junctions in a polarized epithelial model [19, 20]. EAEC strains also often harbor a variable number of serine protease autotransporters of Enterobacteriaceae (SPATEs) that are implicated in immune evasion, mucosal damage, secretogenicity, and colonization [21].

Received 28 January 2014; accepted 11 June 2014; electronically published 18 July 2014.

Correspondence: Nadia Boisen, PhD, Department of Pediatrics, University of Virginia School of Medicine, P.O. Box 800326, 409 Lane Road, Charlottesville, VA 22908 (nb9f@virginia.edu).

The Journal of Infectious Diseases® 2014;210:1909–19

© The Author 2014. Published by Oxford University Press on behalf of the Infectious Diseases Society of America. All rights reserved. For Permissions, please e-mail: journals.permissions@oup.com.

DOI: 10.1093/infdis/jiu399

In 2011, an outbreak of foodborne hemorrhagic colitis originated in Germany, spreading to other European countries. Over 4000 individuals were affected, including primary and secondary cases [22]. Hemolytic uremic syndrome (HUS) developed in approximately 22% of the cases [22], and 54 people died [23, 24]. The implicated pathogen was an EAEC strain of the rare serotype O104:H4 [23], which was lysogenized with an Stx2a-converting phage. Genomic analysis [25] demonstrated that the outbreak strain contained the genes required to produce the AAF/I variant and 3 SPATEs (Pic, SigA, and SepA). Although much is known about the pathogenesis of serotype O157:H7 Shiga toxin (Stx)-producing *E. coli*, it is unclear how an EAEC strain would be able to elicit severe hemorrhagic colitis and HUS, even when harboring an Stx-encoding gene. In this study, we tested the hypothesis that the plasmid-borne virulence factors of EAEC contributed to the high pathogenicity of the German outbreak strain by promoting strong adherence to the epithelium and/or by opening epithelial tight junctions.

METHODS

Bacterial Strains, Plasmids, and Growth Conditions

The Stx2a-producing O104:H4 strain C227-11 was isolated in Denmark during the outbreak [23]. Bacterial strains and plasmids used in this study are described in Table 1. Strains were grown at 37°C in Luria broth (LB) or Dulbecco's modified Eagle's medium (DMEM) supplemented with 0.45% glucose. Recovery of bacteria was done on MacConkey agar (Mac) or LB agar. When indicated, media were supplemented with kanamycin (Km; 50 µg/mL), carbenicillin (Ca; 100 µg/mL), tetracycline (Tc; 30 µg/mL), streptomycin (Str; 50 µg/mL), penicillin (Pen; 50 µg/mL), chloramphenicol (Cm; 30 µg/mL), gentamicin (Gm; 100 µg/mL), and/or 0.2% arabinose.

Plasmid and Strain Constructions

Oligonucleotides used are listed in Table 1. Phusion Flash (Fermentas, Waltham, MA) and EasyA (Agilent, Santa Clara, CA) high-fidelity DNA polymerases were used for polymerase chain reaction (PCR) analysis. To obtain a construct expressing *aggDCBA* from an arabinose-inducible promoter, a Cm cassette was amplified from pACYC184 with primers AH1036/1037 and cloned into the pBAD24 *XmnI* site (pAMH187); *aggDCBA* amplified from C227-11 genomic DNA with *aggBADF/aggBADR* primers was ligated into the pAMH187 *NheI/SalI* sites. A complementation plasmid with *aggR* expressed from its native promoter was generated by cloning a DNA fragment amplified from C227-11 genomic DNA, using primers AH1044/AH1045, into the pACYC184 *XmnI* site (pAMH188). An *aggR* mutant was generated by cloning a Km cassette, amplified from pACYC177 with primers AH1056/AH1057, into an *XmnI* site in *aggR* (pAMH189); the *aggR::km*-containing DNA fragment was amplified from pAMH189 with primers AH1083/AH1084 and cloned into the pSRS1 *NdeI/SacI* sites

(pAMH195). Suicide vectors used to generate *aggA* and *sepA* deletion mutants were constructed as follows. DNA fragments containing *aggA* or *sepA* and approximately 500–600-bp flanking sequences were amplified with AH1059/AH1214 and AH1070/AH1215 and cloned into pCR2.1-TOPO with the pENTR/D-TOPO cloning kit (Invitrogen, CA). Reverse-transcription PCR analysis was performed on the resultant plasmids to delete *aggA* and *sepA* with primers AH1178/AH1179 and AH1180/AH118. Amplified DNA was digested with *NruI* and religated with a Km cassette amplified as described above to yield pAMH196 and pAMH198. DNA fragments containing $\Delta aggA::km$ and $\Delta sepA::km$ were amplified from pAMH196 with AH1059/AH1214 and from pAMH198 with AH1070/AH1215, respectively, and cloned into the pSRS1 *XmnI* site to yield pAMH197 and pAMH199. C227-11 deletion and insertion mutants were constructed by allelic exchange as described elsewhere [29]. C227-11 cured of pAA (C227-11/pAA⁻) was generated by electroporation.

Biofilm Assay

Biofilm assay was performed as described previously [30].

Epithelial Cell Infections

Human colonic T84 epithelial cells (ATCC CCL-248) were maintained in DMEM/F-12 medium (Invitrogen, Carlsbad, CA) with 10% fetal bovine serum (FBS; Sigma, St. Louis, MO), and 50 µg/mL Pen/Str. Polarized and nonpolarized T84 cells were grown as described elsewhere [19]. Prior to inoculation, polarized cells in 12-well transwell plates were washed 3 times with Hank's balanced salt solution (HBSS). One milliliter of F-12 medium was added to the basolateral chamber and the apical side of each transwell, followed by incubation at 37°C in 7% CO₂ for up to 1 hour. Medium was then aspirated from the apical compartment, 200 µL of 2–4 × 10⁸ colony-forming units (CFU)/mL bacteria were added, and monolayers were incubated for a further 3 hours. Monolayers were then washed, and medium was replaced with fresh medium containing 100 µg/mL Gm and incubated for a further 24 hours. Transepithelial electrical resistance (TEER) was measured at 3, 18, and 24 hours, using an ohmmeter (World Precision Instruments, Sarasota, FL).

For the T84 adherence assay, 50 µL of the bacterial suspension were added to confluent monolayers in a 24-well plate and incubated at 37°C in 7% CO₂ for 3 hours. Cells were washed 3 times with HBSS and incubated with 500 µL of 1% Triton X-100 in phosphate-buffered saline (PBS) for 30 minutes at room temperature. The medium was serially diluted and plated. To calculate the percentage recovery of adherent bacteria, bacteria were enumerated by colony counts before and after the infection period.

Vero Cell Cytotoxicity Assay

Vero cell cytotoxicity assays were performed as described elsewhere [31, 32].

Table 1. Strains, Constructs, and Oligonucleotides Used in This Study

Strain, Plasmid, or Oligonucleotide	Genotype and/or Relevant Characteristic(s)	Reference
Strain		
C227-11	Wild-type O104:H4 Stx2a-producing strain	[23]
C227-11 ϕ cu	C227-11 cured of Stx2a encoding phage	[31]
C227-11/pAA ⁻	C227-11 cured of the pAA plasmid	This study
C227-11 Δ aggR	C227-11 with the insertion mutation <i>aggR::km</i> , Km ^r	This study
C227-11 Δ aggA	C227-11 with the insertion deletion Δ <i>aggA::km</i> , Km ^r	This study
C227-11 Δ sepA	C227-11 with the insertion deletion Δ <i>sepA::km</i> , Km ^r	This study
86-24	EHEC O157:H7 Stx-producing strain	[46]
S17- λ pir	λ pir lysogen of <i>E. coli</i> K12 strain S17-1	[47]
HB101	<i>E. coli</i> K12/B hybrid strain	Gibco
DH5 α	<i>E. coli</i> K12 strain	Invitrogen
HS	Human commensal <i>E. coli</i> strain	[48]
Plasmid		
pCR2.1-TOPO	TOPO TA cloning vector, Km ^r Amp ^r	Invitrogen
pACYC177	Medium-copy-number cloning vector, Km ^r Amp ^r	New England Biolabs
pACYC184	Medium-copy-number cloning vector, Cm ^r Tc ^r	New England Biolabs
pBAD24	Expression vector containing an arabinose-inducible promoter	[49]
pSRS1	Suicide vector derivative of pJMM112, <i>sacB</i> , Amp ^r	[50]
pAMH187	pBAD24:: <i>cm</i> , Cm ^r	This study
pAMH188	pACYC184:: <i>aggR</i> , Cm ^r	This study
pAMH189	pAMH188 with a km ^r cassette inserted into <i>aggR</i> , Cm ^r Km ^r	This study
pAMH192	pBAD24:: <i>cm::aggDCBA</i> , Cm ^r	This study
pAMH195	pSRS1:: <i>aggR::km</i> , Km ^r	This study
pAMH196	pCR2.1-TOPO:: <i>aggA::km</i> , Km ^r	This study
pAMH197	pSRS1:: <i>aggA::km</i> , Km ^r	This study
pAMH198	pCR2.1-TOPO:: <i>sepA::km</i> , Km ^r	This study
pAMH199	pSRS1:: <i>sepA::km</i> , Km ^r	This study
Oligonucleotide, sequence (5'–3')		
aggBADF	CGTACGCTAGCAGGAGGAATTCACCATGCTTTATAAGCCGAATCTTCTGGAGA	This study
aggBADR	CGTACGCTGACTTAAAAATCAACTGCAGCATGGAGTATCATTGT	This study
AH1036	CAAGGATCCAAGCTTGCGCCGAATAAATACCTGTGAC	This study
AH1037	CAAGGATCCAAGCTTATTACTTATTCAGGCGTAGCACCA	This study
AH1044	GACTGGGCTGCAATTAAGATACAAC	This study
AH1045	GCTTACGTGCTTGATAAGTATAAGTGAG	This study
AH1056	CATCATCCAGCCAGAAAGTGAGG	This study
AH1057	GTCAAGTCAGCGTAATGCTCTGC	This study
AH1059	CGTACTCGAGGAAGCTGATGCTGCAGCTATATGTG	This study
AH1070	CGTCAGCTGGCATTGGCTTTACGCTTACGTGA	This study
AH1083	CGTACATATGACTGGGCTGCAATTAAGATACAAC	This study
AH1084	CGTCAGCTGCTTACGTGCTTGATAAGTATAAGTGAG	This study
AH1178	GCACTCGCGAGCATGCTCCGATCATTGATTGGCAT	This study
AH1179	GCACTCGCGATGTGTTTTACCTATTGATATTGACATTGT	This study
AH1180	GCACTCGCGAGAATGGGATAGGCCCTGCCAT	This study
AH1181	GCACTCGCGAGGAGCAGTCCGAGATTCTACTAATATCA	This study
AH1214	CACCCATATGAAGAGCATATTACCGATGTCCTGCG	This study
AH1215	CACCCATATGCATAAGGACTGACTGAATCGTGC	This study

Abbreviations: Amp, ampicillin; Cm, chloramphenicol; *E. coli*, *Escherichia coli*; Km, kanamycin; Tc, tetracycline.

Organ Culture Adhesion Assay With Tissue From *Macaca fascicularis*

A cynomolgus monkey explant model based on the method of Hicks et al [33] was developed. A veterinarian performed

necropsy of the animal and harvested 10-cm sections of the colon. Fecal matter was removed by PBS washes. Ten-millimeter biopsy specimens were generated with an Acu Punch device (Acuderm, Fort Lauderdale, FL); the sections were oriented

with the mucosal surface facing up in 48-well tissue culture plates. The tissue was saturated with F-12 medium mixed with NCTC-135 medium (1:1) with 10% FBS, and 50 μ L of the bacterial culture (C227-11, 7.4×10^8 CFU/mL; C227-11/pAA⁻, 9×10^8 CFU/mL; and HS, 2.4×10^9 CFU/mL) were added to the mucosal surface of the specimens. The tissues were incubated with the bacteria at 37°C in 5% CO₂ for 3 hours, and bacteria were recovered on Mac agar supplemented with Ca/Tc (C227-11 and C227-11/pAA⁻) and Str (HS). The experiment was done in triplicate.

Tissue or Biofilm Processing for Scanning Electron Microscopy (SEM)

SEM of samples was done at the Core Imaging Facility, University of Maryland Dental School, Baltimore. For biofilm assessment, cultures were grown overnight on glass coverslips in 24-well plates. Tissue and biofilm samples were washed 3 times with PBS and fixed in 2% paraformaldehyde/2.5% glutaraldehyde in PBS. Specimens were coated with gold in a sputter coater (EMS 350), and images were taken with Quanta 200 (FEI, Hillsboro, OR) as specified by the manufacturer.

Confocal Microscopy Imaging

Cells were fixed and permeabilized in 4% paraformaldehyde in PBS prior to DNA (nuclear) staining with Hoechst 33342 (Invitrogen). Actin was stained with Alexa Fluor 633 phalloidin (Invitrogen). Cells were imaged using a Zeiss 210 Confocal Microscope (original magnification, 40 \times).

Statistical Analyses

Statistical analyses were performed using GraphPad Prism v6.00 (GraphPad Software, San Diego, CA), and results are specified in figure legends.

Interleukin 8 (IL-8) Enzyme-Linked Immunosorbent Assay

IL-8 secretion was measured from polarized T84 cells in triplicate, as described by Harrington et al [20], at the Cytokine Core Laboratory at the University of Maryland, Baltimore.

RESULTS

Plasmid pAA of C227-11 Is Important for Adherence to Monkey Intestinal Explants

We used a cynomolgus monkey explant model to observe histopathologic changes and measure mucosal adherence by C227-11. Monkey colonic tissue was infected with C227-11, C227-11/pAA⁻, or the commensal *E. coli* strain HS. Adherence of C227-11/pAA⁻ and HS to monkey tissue was significantly less ($P < .0072$) than that observed for wild-type (wt) C227-11 (Figure 1A). As was reported for human intestinal explants infected with EAEC [33], SEM revealed dilatation of the crypts, loss of the normal mucus layer, and adherence by C227-11 in both aggregates and singletons after 3 hours of infection (Figure 1D and 1E). No dilatation was observed with HS (Figure 1C).

Adherence of C227-11 Is AAF Dependent

We next characterized the capacity of C227-11 and mutants deleted for the pAA genes *aggR*, *aggA*, and *sepA* to adhere to T84

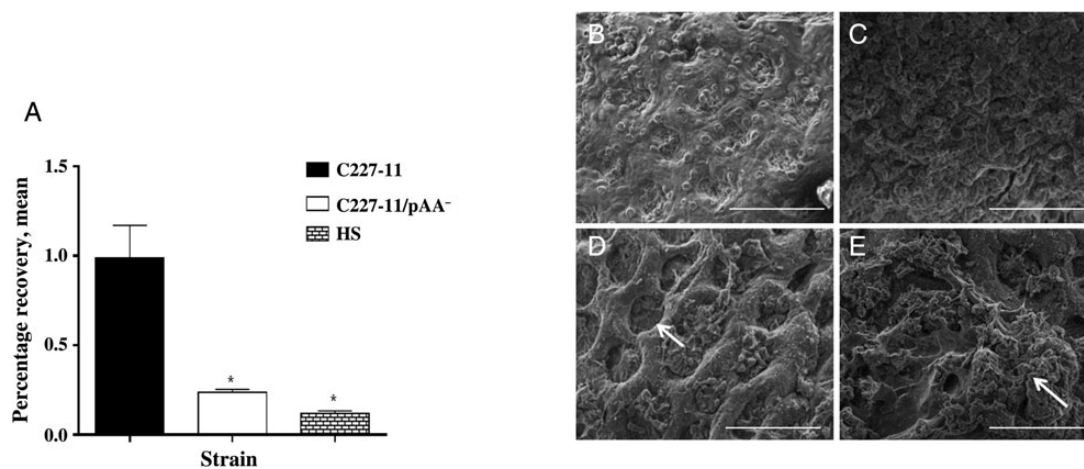


Figure 1. Adherence to *Macaca fascicularis* intestinal explants. Sections of proximal colon from freshly euthanized cynomolgus monkeys (A) were incubated with C227-11, C227-11/pAA⁻, or HS for 3 hours on selective medium and homogenized, and bacteria were enumerated (C227-11, 7.33×10^6 adherent colony-forming units [CFU]/mL; C227-11/pAA⁻, 2.13×10^6 adherent CFU/mL; HS, 2.85×10^6 adherent CFU/mL); percentage recovery was calculated. The bars represent the mean from triplicate wells; error bars indicate 1 SD. * $P < .05$ and ** $P < .001$, by analysis of variance with the Tukey post hoc test, for comparison between C227-11 and C227/pAA⁻ or HS. B–E, Sections of proximal colon from freshly euthanized cynomolgus monkeys were incubated with medium alone (B), with HS (C), or with strain C227-11 for 3 hours (D and E) and then viewed by scanning electron microscopy. In panel D, the arrow indicates dilatation of the crypts, and in panel E, the arrow indicates aggregating bacteria. Scale bar is 100 μ m. Abbreviation: SD, standard deviation.

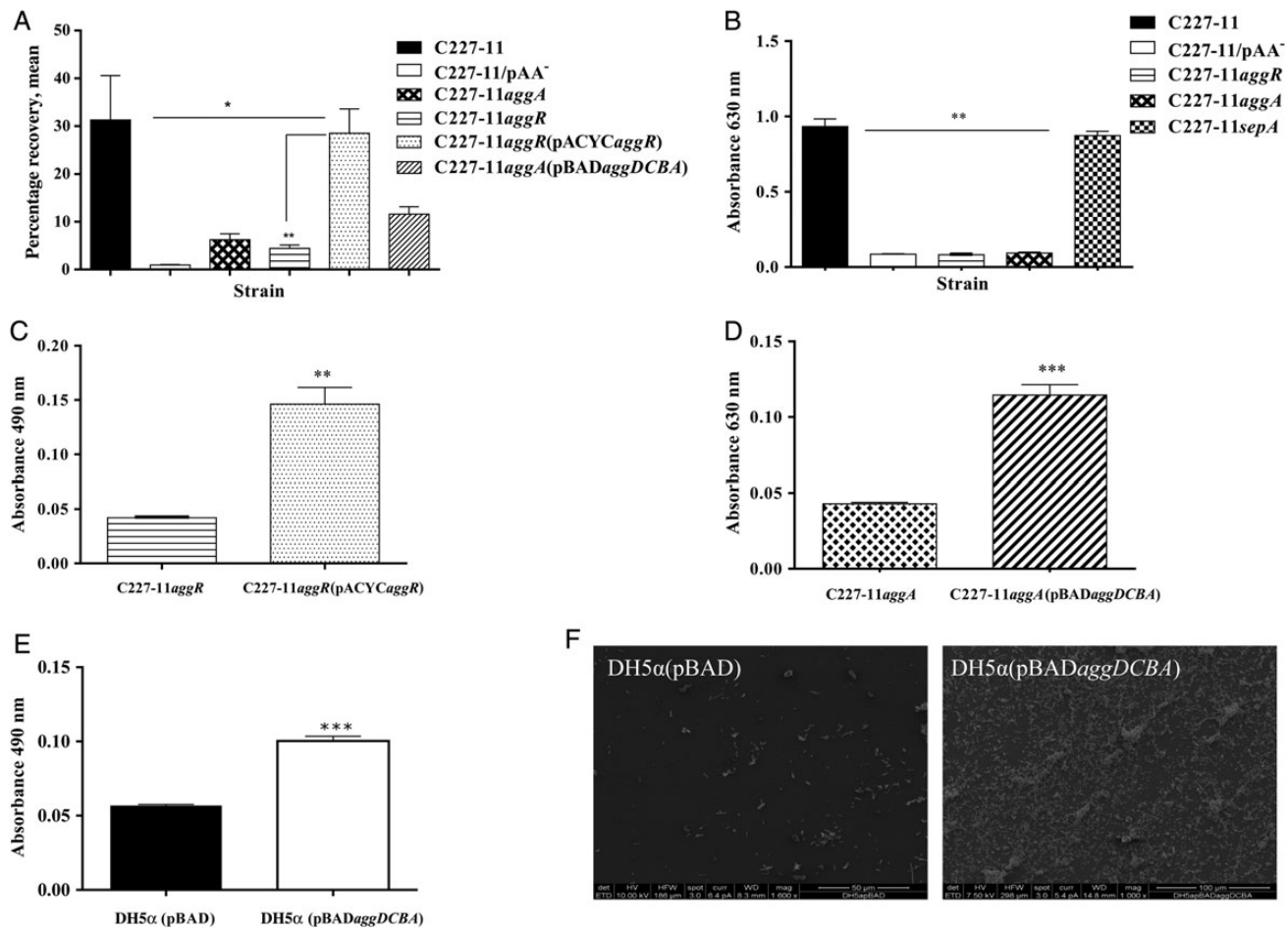


Figure 2. T84-cell adherence and biofilm formation of C227-11; mutants C227-11/pAA⁻, C227-11*aggR*, C227-11*aggA*, and C227-11*sepA*; and complemented strains C227-11*aggR*(pACYC*aggR*) and C227-11*aggA*(pBAD*aggDCBA*). *A*, Adherence of C227-11 and mutants to T84-cell monolayers after incubation for 3 hours. **P* < .05, by analysis of variance (ANOVA) with the Tukey correction, for comparison between wild-type and mutant strains. ***P* < .001 for comparison between C227-11*aggR* and the complemented strain. *B–E*, Quantification of biofilm formation over 20 hours by C227-11 and mutants (*B*; ***P* < .001, by ANOVA with the Tukey post hoc test, between wild-type and all mutant strains), C227-11*aggR* and C227-11*aggR*(pACYC*aggR*) (*C*), C227-11*aggA* and C227-11*aggA*(pBAD*aggDCBA*) (***) *P* < .0001, by an unpaired *t* test with the Welch correction; *D*), and DH5α(pBAD) or DH5α(pBAD*aggDCBA*) (*E*). *F*, Scanning electron microscopy of DH5α(pBAD) and DH5α(pBAD*aggDCBA*) grown overnight on glass coverslips. Bars represent an average of ≥3 separate experiments with each done in triplicate. Error bars represent 1 SD. Abbreviation: SD, standard deviation.

cells and to form biofilms on plastic surfaces. C227-11 adhered to T84 cells and formed a biofilm similar to that formed by other EAEC strains described, whereas deletion of *aggA* or *aggR* significantly attenuated the capacity of C227-11 to adhere to polarized T84 cells (*P* < .0008; Figure 2*A*) and to form a biofilm (*P* < .0001; Figure 2*B*). Adherence to T84 cells and biofilm formation were restored when C227-11*aggR* (*P* < .0074; Figure 2*C*) or C227-11*aggA* (*P* < .0001; Figure 2*D*) were complemented with the corresponding genes, indicating that the biofilm-forming capacity of C227-11 is mediated by AAF and that AAF expression in C227-11 is regulated by *AggR*. Deletion of *sepA* did not affect biofilm formation (Figure 2*A*).

The phenotype conferred by AAF/I was further evaluated by transforming the operon that encodes AAF/I into *E. coli* K12 strain DH5α and testing the strain for biofilm formation.

DH5α(pBAD*aggDCBA*) formed heavy biofilms, while DH5α with the vector alone (DH5α[pBAD]) did not (*P* < .0001; Figure 2*E*). The biofilm formed by DH5α(pBAD*aggDCBA*) comprised thick aggregates (Figure 2*F*) with the classic aggregative adherence pattern typically observed for EAEC, while DH5α(pBAD) did not form aggregates.

AggR Is Required for C227-11–Mediated Morphologic Changes in the Cytoskeleton of T84 Cells

Both Shiga toxin-producing *E. coli* (STEC) and EAEC strains induce actin rearrangements in epithelial cells. We speculated that C227-11 adherence might lead to rearrangement of host cell actin and assayed for this phenotype by fluorescence actin staining. We found that although actin was organized as expected in uninfected T84 cells (Figure 3*A–C*), cells with adherent

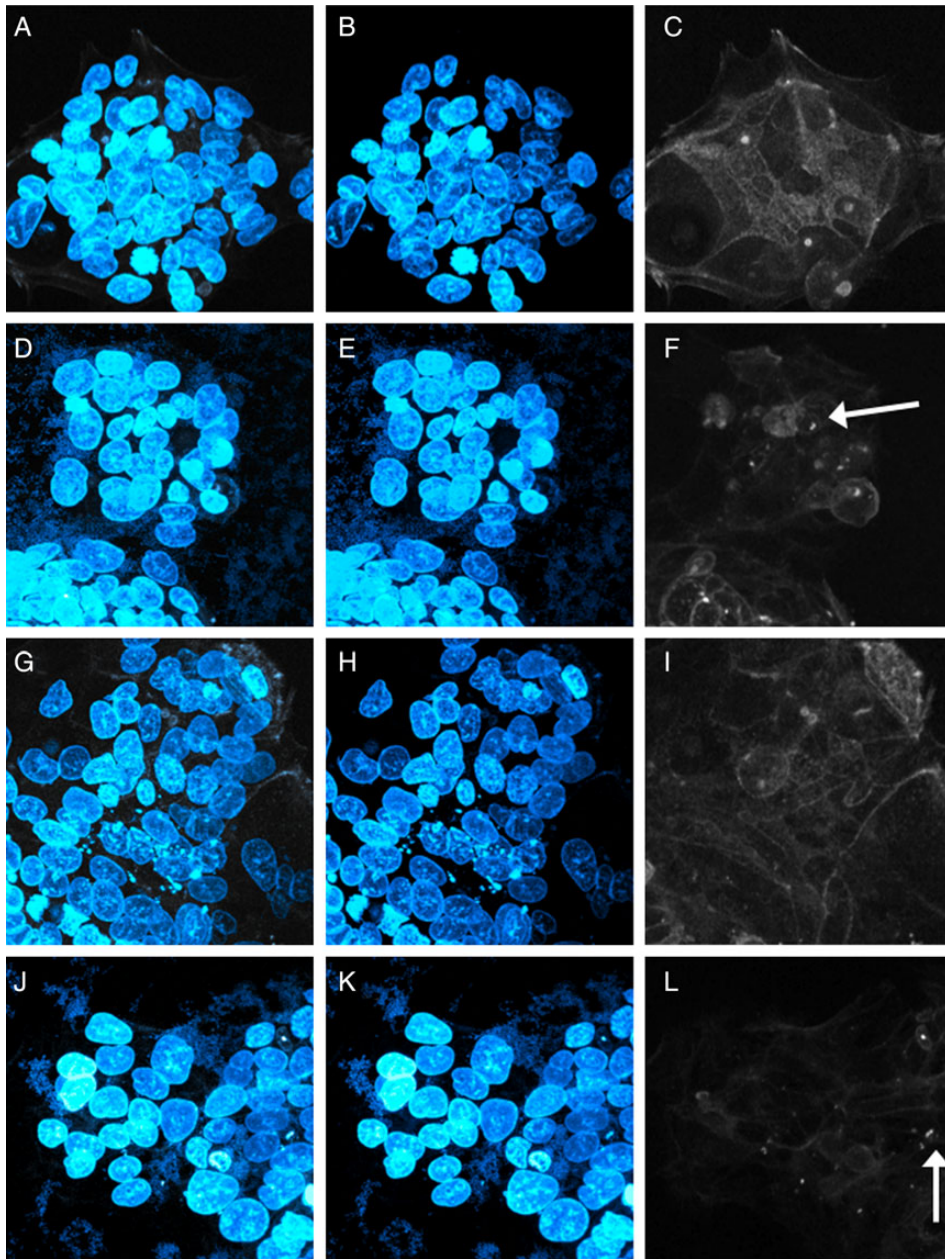


Figure 3. Strain C227-11 causes disruption in the cytoskeleton of T84 cells. Enteroaggregative *Escherichia coli* strains were co-cultured with polarized T84-cell monolayers for 3 hours, then visualized with epifluorescence microscopy. The cell nuclei and bacterial DNA were stained with Hoechst 33324 (blue), and the cellular actin was stained with phalloidin 633 (white). *A, D, G, and J*, Overlaid images with both Hoechst 33324 and phalloidin stain. *B, E, H, and K*, Images showing Hoechst 33324 staining. *C, F, I, and L*, Images showing staining with phalloidin 633 alone. *A–C*, T84-cell control without added bacteria. *D–F*, C227-11 wild-type strain cocultured with T84 cells. *G–I*, C227-11 *aggR* cocultured with T84 cells. *J–L*, C227-11 *aggR*(pACYC*aggR*) cocultured with T84 cells. Arrow indicates condensed actin.

C227-11 exhibited disruption and disorganization of the actin cytoskeleton (Figure 3*D–F*). In contrast, cells infected with the *aggR* mutant (Figure 3*G–I*) showed no adherent bacteria and less disruption of actin microfilaments; the wt phenotype was restored by complementing the *aggR*-deleted strain with pACYC*aggR* (Figure 3*J–L*)

C227-11 Disrupts Polarity (TEER) of a T84-Cell Monolayer

EAEC strains elicit decreased barrier function [19]. To characterize the effects of C227-11 on intestinal barrier function, we measured the TEER of polarized T84-cell monolayers infected with C227-11, C227-11/pAA⁻, HS, EAEC prototype 042, or O157:H7 STEC strain 86-24. After infection for 3 hours, the

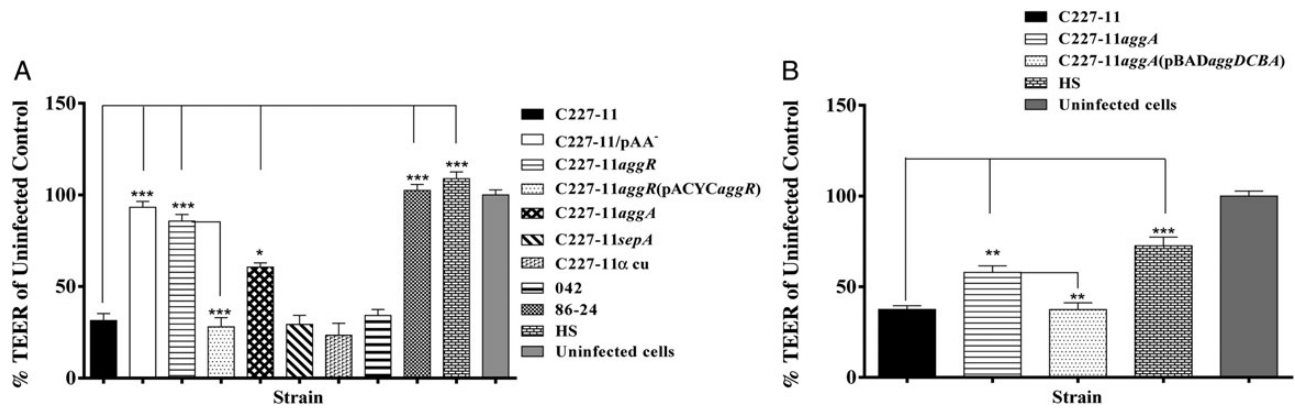


Figure 4. Strain C227-11 induces barrier disruption. *A* and *B*, Polarized T84 cells were infected with enteroaggregative *Escherichia coli* (EAEC) strain C227-11, mutants C227-11/pAA⁻, C227-11*aggR*, C227-11*aggA*, C227-11*sepA*, C227-11 Φ cu, C227-11*aggR*(pACYC*aggR*), or HS (*A*), or C227-11, C227-11*aggA*, C227-11*aggA*(pBAD*aggDCBA*), or HS (*B*). Shiga toxin–producing *E. coli* O157:H7 86-24 served as a negative control and EAEC strain 042 as positive control for barrier disruption, and commensal *E. coli* strain HS and uninfected monolayers served as negative controls. Three hours after the addition of bacteria, the infection was terminated by aspiration of the apical compartment medium and addition of fresh medium containing gentamicin. Transepithelial electrical resistance (TEER) was measured 18 hours after infection and reported as the percentage of the initial value. The data represent an average of 3 separate experiments, with each performed in triplicate. Error bars indicate 1 SD from the mean TEER. **P* < .05, ***P* < .001, and ****P* < .0001, by analysis of variance with the Tukey post hoc test, for comparison between C227-11, mutants, and complemented mutants. Abbreviation: SD, standard deviation.

monolayers were washed, and fresh medium containing Gm was added; TEER was measured at intervals for 24 hours. By 18 hours after infection, the reduction of TEER induced by C227-11 (defined as the percentage of the TEER value of the uninfected monolayer) was significant, compared with uninfected monolayers and those infected with HS, C227-11/pAA⁻, or STEC strain 86-24 (Figure 4*A*). We observed no difference in TEER between 18 hours and 24 hours.

Effects of C227-11 on TEER Requires *AggR* and *AggA* but Not *SepA* or *Stx2a*

To ascertain the genes involved in reduced monolayer resistance induced by C227-11, we tested the *aggR*, *aggA*, and *sepA* mutants, as well as a mutant cured of the phage encoding Stx2a (C227-11 Φ cu [26]). C227-11*aggR* and C227-11*aggA* did not increase T84 barrier permeability, as measured by TEER (Figure 4*A*). However, complementation of either mutant restored the capacity to reduce TEER (Figure 4*A* and 4*B*). C227-11*sepA* and C227-11 Φ cu induced alteration of barrier function similar to the wt strain, suggesting that disruption of the intestinal barrier by C227-11 does not require *SepA* or *Stx2a* but is either mediated directly by AAF/I or constitutes an effect augmented by the adhering bacteria.

C227-11 Causes IL-8 Release

Proinflammatory cytokines IL-8 and interleukin 1 β (IL-1 β) can be detected in feces from cases of EAEC-mediated diarrhea [34]. Moreover, polarized T84 cells infected with EAEC strain 042 mutated in *aafA*, the major pilin subunit of the AAF/II cluster, released significantly less IL-8 than cells infected with

wt 042 [20]. To assess this phenotype for Stx-EAEC, we collected the basolateral supernatants from infected and Gm-treated polarized T84 cells at the end of the 24-hour period and analyzed the samples for the cytokines IL-8, interleukin 6, IL-1 β , interleukin 10, interleukin 12p70, and tumor necrosis factor α . IL-8 secretion was induced from polarized T84 cells infected with C227-11, compared with the uninfected control and C227-11/pAA⁻ (Figure 5*A*), suggesting that factors on the pAA plasmid of C227-11 contribute to EAEC-induced inflammation. We next assessed C227-11 and the panel of mutants for the capacity to induce IL-8 from the polarized T84 cells. We found that deletion of *aggR*, *aggA*, *sepA*, or the Stx2a-encoding phage from C227-11 induced significantly less IL-8 release from the cells, compared with the wt strain (*P* < .0001; Figure 5*A*). Complementation of C227-11*aggR* restored IL-8 release to levels of the wt strain. Complementation of C227-11*aggA* with the fimbrial cluster did not restore IL-8 release to wt levels; however, polarized T84 cells infected with *aggDCBA* transformed into HB101 demonstrated IL-8 release (Figure 5*B*), indicating that the AAF/I-encoding *agg* fimbrial cluster from C227-11 is sufficient to induce an inflammatory response or that disruption of tight junctions causes such a release.

Plasmid pAA and *AggA* Augment Translocation of *Stx2a*

To investigate whether C227-11 pAA-encoded genes are important for translocation of Stx2a in the polarized T84-cell model, we assayed for Stx2a-induced cytotoxic activity in the same basolateral medium in which IL-8 was measured. We found significantly more Stx2a on the basolateral side of cells infected with C227-11, compared with the strains without pAA (*P* < .0001), *aggR*

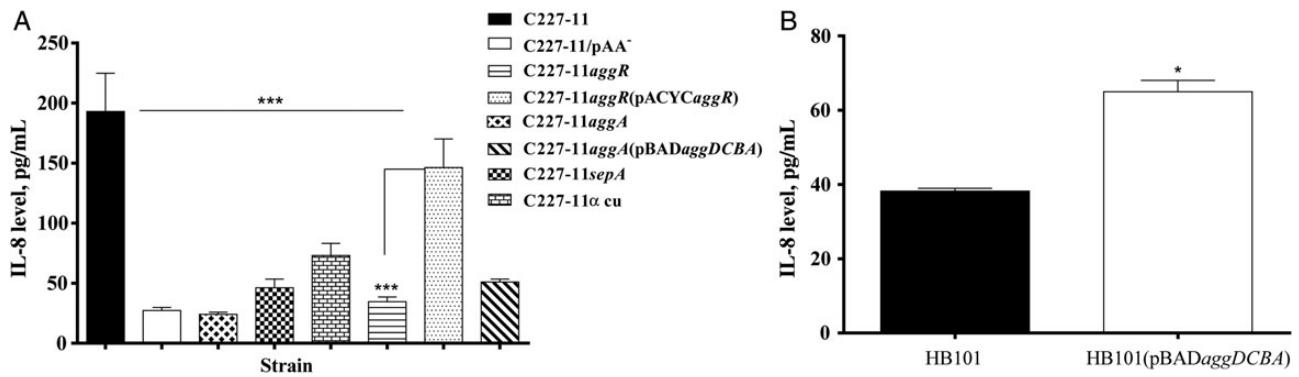


Figure 5. Strain C227-11 induces interleukin 8 (IL-8) release from T84 cells. *A*, IL-8 levels in supernatants from the basolateral compartments of polarized T84 cells infected with C227-11, C227-11/pAA⁻, C227-11aggR, C227-11aggR(pACYCaggR), C227-11aggA, C227-11sepA, or C227-11Φcu. ****P* < .0001, by analysis of variance with the Tukey post hoc test, for comparison between C227-11, mutants, and complemented strains. *B*, IL-8 levels in supernatants from the basolateral compartments of polarized T84 cells infected with *Escherichia coli* strain HB101 with or without the *aggDCBA* fimbrial cluster from C227-11. **P* < .0139, by the unpaired *t* test with the Welch correction. Bars show mean IL-8 levels, as measured by enzyme-linked immunosorbent assay, from an average of 3 separate experiments, with each done in triplicate. Error bars represent 1 SD. Abbreviation: SD, standard deviation.

(*P* < .0001), or *aggA* (*P* < .05). *SepA* has not previously been studied in EAEC. Deletion of *sepA* caused a nonsignificant (*P* = .15) reduction of cytotoxicity, compared with C227-11 (Figure 6*A*). Notably, when we complemented the *aggR* mutant with *aggR* in trans, Stx2a translocation was restored to wt levels (Figure 6*A*). Last, no Stx2a could be detected from the basolateral side of monolayers infected with STEC strain 86-24 (data not shown).

We next investigated whether the C227-11 fimbrial cluster *aggDCBA* expressed in a K12 background promotes the translocation of Stx2a across polarized T84 cells. We applied 500 ng/mL of Stx2a to the apical surface of polarized T84 monolayers and to monolayers infected with DH5α(pBAD) or DH5α

(pBADaggDCBA). We found that Stx2a translocation was significantly more efficient in monolayers infected with DH5α (pBADaggDCBA), compared with DH5α(pBAD) (*P* = .0396; Figure 6*B*), indicating that expression of AAF alone is sufficient to enhance delivery of the toxin across the epithelium.

DISCUSSION

Much is known about the pathogenesis of EAEC infection, although how the factors of EAEC would be sufficient to confer virulence in the presence of Stx remains obscure. To elucidate characteristics of this strain, we developed a colonic explant

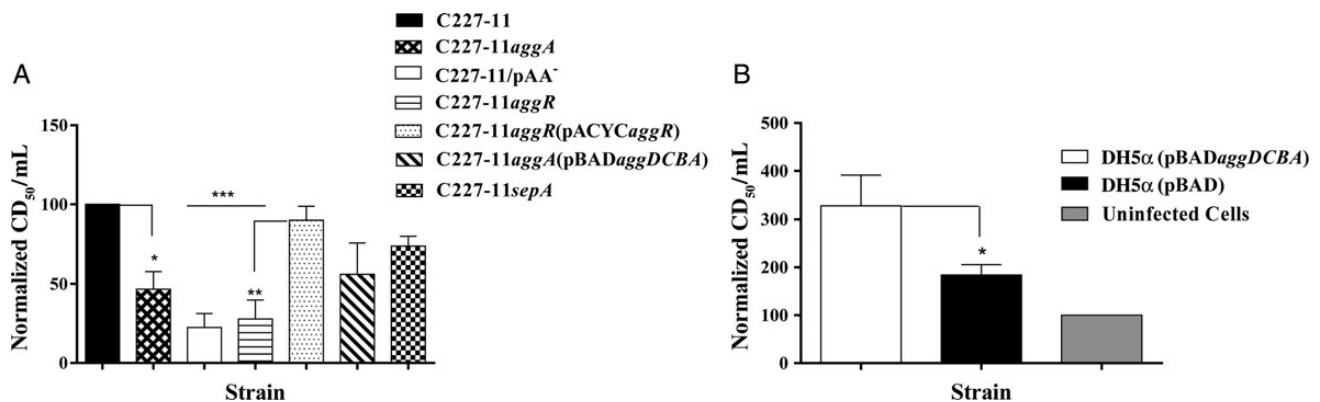


Figure 6. Strain C227-11 adherence promotes translocation of Shiga toxin type 2a (Stx2a) across T84 monolayers. Supernatants from the basolateral compartment of polarized monolayer dishes were collected 24 hours after infection, and the cytotoxicity (CD₅₀) per milliliter was determined on Vero cells. Bars show the mean CD₅₀ from at least 3 separate experiments, with each done in triplicate. *A*, The CD₅₀ values were normalized such that the sample from C227-11 was set to 100. **P* < .05, ***P* < .001, and ****P* < .0001, by analysis of variance with the Tukey post hoc test, for comparison between C227-11, mutants, and complements. *B*, DH5α(pBADaggDCBA) and DH5α were incubated with 500 ng/mL of Stx2a during the 3-hour period of T84-cell infection. **P* < .0396, by a 1-tailed unpaired *t* test, for comparison between DH5α(pBADaggDCBA) and DH5α(pBAD). Bars show mean CD₅₀ levels, as determined on Vero cells in a representative experiment, with each experiment done in triplicate. Error bars represent 1 SD. Abbreviation: SD, standard deviation.

model, using tissue from cynomolgus monkeys. In this model and on polarized T84 cells, we found that the C227-11 pAA plasmid and its AAF were necessary for adherence, as shown for EAEC strains on human explants [33]. We further found that pAA and AggA are required for biofilm formation, disruption of TEER in polarized T84 cells, and release of IL-8 from those T84 cells. This is consistent with other studies suggesting that colonization of intestinal epithelium occurs by virtue of the AAF [14–16, 18] and that the adhesin itself is sufficient to confer not only adherence but also release of IL-8 from epithelial cells and opening of intestinal tight junctions [19]. Our data suggest a new function for pAA: promotion of Stx2a penetration through polarized T84 cells. This is also consistent with a study by Tran et al, who reported that the increased virulence of the German outbreak strain is not attributed to increased Stx expression and transcytosis [35].

Studies have reported that purified Stx2a crosses from the apical side to the basolateral side of T84 cells without destroying cells or altering tight junctions [36, 37]. Interestingly, adherence by STEC O157:H7 strain 86-24 did not disrupt a polarized T84-cell monolayer and did not cause appreciable levels of Stx2a to cross that monolayer. In contrast, infection of T84 cells with C227-11 allowed significant levels of Stx2a to reach the basolateral side of the monolayer. We also observed this effect with the Finnish O104:H4 isolate C68-11 [23, 25] (data not shown). We observed that disruption of T84-cell polarization is independent of Stx2a, since the Stx2a-negative strain C227-11 ϕ cu caused disruption of TEER in polarized T84 cells at a level similar to that caused by its parent, C227-11. Since Stx absorption from the gut to the systemic circulation is a crucial step in the pathogenesis of clinical complications following STEC infection [38], it is possible that the capacity of C227-11 to disrupt polarized cells and deliver toxin across those cells may have contributed to the severity of disease observed in the German outbreak.

Disruption of the epithelial barrier has been shown to coincide with perturbation of the actin cytoskeleton for STEC strains that carry the locus of enterocyte effacement (LEE) island [39, 40]. Cytoskeletal rearrangement has been demonstrated for EAEC and linked to the presence of both the AAF [19] and the Pet toxin [41], a toxin that is not found in C227-11. We report here that deletion of *aggR* from strain C227-11, which does not harbor the LEE, caused a reduction in actin rearrangement in T84 cells. Thus, the contribution of *aggR* in altering actin arrangement (and reducing adherence) is likely due to its role in the expression of AAF/I. We also observed that incubation of C227-11 with polarized T84 cells induced IL-8 secretion and that cytokine release was significantly lower when the cells were infected with C227-11 Φ cu, a finding that indicates that Stx2a contributes to cytokine release. Others have reported that purified Stx causes IL-8 release from intestinal epithelial cells [42]. In addition, deletion of *aggA*, *aggR*, and *sepA* significantly decreased secretion of IL-8 into the basolateral

compartment (Figure 5). SepA is associated with increased mucosal inflammation in *Shigella* infection [43] and may have cytotoxic effects of its own. However, we did not observe cytotoxic effects associated with the presence of SepA in the T84-cell assay. The contribution of SepA to Stx-EAEC virulence remains unknown.

We have shown that polarized T84 cells infected with HB101 transformed with *aggDCBA* demonstrated increased IL-8 release, compared with HB101 alone (Figure 5B), a result that suggests that the *agg*-fimbrial cluster from C227-11 is sufficient to induce a proinflammatory response, as previously reported for the EAEC AAF/I prototype strain, JM221 [44]. Although flagella may contribute to the inflammatory response in EAEC infection, we have previously reported that this effect is minimal in polarized T84 cells (compared with nonpolarized monolayers) and that it is less than the contribution of the AAFs [20]. Notably, Hurley et al speculated that the degree of intestinal inflammation may correlate with Stx penetration for STEC, and our data are compatible with that model [45]. Thus, the colitis induced by the German outbreak strain may have been caused by a combined effect of Stx and the proinflammatory effectors of EAEC, including the AAF adhesin.

Perhaps the most important observation of our study was that the AAF fimbrial adhesin expressed in a K12 background was sufficient to enhance translocation of Stx2a across the epithelial monolayer. Since the toxin was applied independently, rather than expressed by DH5 α (pBAD*aggDCBA*), enhanced translocation was apparently due to a direct effect of the adhesin on epithelial permeability. The increased translocation is presumably related to the previously described ability of AAF to disrupt epithelial tight junction proteins [19], but this is not proven by our experiments, and it is notable that the reduction in TEER alone is apparently not sufficient to enhance translocation of Stx by STEC.

The report of a large and severe outbreak of colitis and HUS attributed to an Stx-EAEC strain raises questions about how the virulence factor of one pathotype (STEC) can realize an effective partnership with a package of virulence factors from a different pathotype (EAEC). The findings presented here support the importance of the pAA plasmid in the pathogenesis of the O104:H4 outbreak strain, both in ways typical of EAEC (adherence and inflammation) and in a unique and sinister new synergy (barrier dysfunction augmenting Stx translocation). Consistent with our findings, Zhang et al reported that loss of the pAA plasmid reported in the course of the disease might have attenuated virulence and diminished the capacity of the strain to cause HUS [27]. Nevertheless, Munera et al reported that pAA is dispensable for rabbit colonization by Stx-EAEC [28]. Taken together, our data suggest that the pAA plasmid of the German outbreak strain may have contributed to the virulence of this strain in multiple ways. Given this combination of traits, it will be of more than passing interest to remain vigilant for the reoccurrence of this highly virulent pathogen.

Notes

Acknowledgments. We thank Dr Aruna Panda, University of Maryland, for providing the colon explant tissue; Prof O. Colin Stine, University of Maryland, for laboratory support; and Dr Jennifer Morrell-Falvey, Oak Ridge National Laboratory, for assistance with confocal microscopy.

Financial support. This work was supported by the National Institutes of Health (grants AI-033096 to J. P. N., DK-058957 to J. B. K., AI-021657 to J. B. K., and AI-020148 to A. D. O.) and the Uniformed Services University (grant R0731977 to A. D. O.).

Potential conflicts of interest. All authors: No reported conflicts.

All authors have submitted the ICMJE Form for Disclosure of Potential Conflicts of Interest. Conflicts that the editors consider relevant to the content of the manuscript have been disclosed.

References

- Adachi JA, Jiang ZD, Mathewson JJ, et al. Enteroaggregative *Escherichia coli* as a major etiologic agent in traveler's diarrhea in 3 regions of the world. *Clin Infect Dis* **2001**; 32:1706–9.
- Okeke IN, Lamikanra A, Steinrück H, Kaper JB. Characterization of *Escherichia coli* strains from cases of childhood diarrhea in provincial southwestern Nigeria. *J Clin Microbiol* **2000**; 38:7–12.
- Fang GD, Lima AA, Martins CV, Nataro JP, Guerrant RL. Etiology and epidemiology of persistent diarrhea in northeastern Brazil: a hospital-based, prospective, case-control study. *J Pediatr Gastroenterol Nutr* **1995**; 21:137–44.
- Bhan MK, Raj P, Levine MM, et al. Enteroaggregative *Escherichia coli* associated with persistent diarrhea in a cohort of rural children in India. *J Infect Dis* **1989**; 159:1061–4.
- Wanke CA, Mayer H, Weber R, Zbinden R, Watson DA, Acheson D. Enteroaggregative *Escherichia coli* as a potential cause of diarrheal disease in adults infected with human immunodeficiency virus. *J Infect Dis* **1998**; 178:185–90.
- Sahl JW, Steinsland H, Redman JC, et al. A comparative genomic analysis of diverse clonal types of enterotoxigenic *Escherichia coli* reveals pathovar-specific conservation. *Infect Immun* **2011**; 79:950–60.
- Valentiner-Branth P, Steinsland H, Fischer TK, et al. Cohort study of Guinean children: incidence, pathogenicity, conferred protection, and attributable risk for enteropathogens during the first 2 years of life. *J Clin Microbiol* **2003**; 41:4238–45.
- Boisen N, Scheutz F, Rasko DA, et al. Genomic characterization of enteroaggregative *Escherichia coli* from children in Mali. *J Infect Dis* **2012**; 205:431–44.
- Lima IFN, Boisen N, Quetz Jda S, et al. Prevalence of enteroaggregative *Escherichia coli* and its virulence-related genes in a case-control study among children from north-eastern Brazil. *J Med Microbiol* **2013**; 62 (Pt 5):683–93.
- Okeke IN, Lamikanra A, Czeczulin J, Dubovsky F, Kaper JB, Nataro JP. Heterogeneous virulence of enteroaggregative *Escherichia coli* strains isolated from children in Southwest Nigeria. *J Infect Dis* **2000**; 181:252–60.
- Boisen N, Ruiz-Perez F, Scheutz F, Krogfelt KA, Nataro JP. Short report: high prevalence of serine protease autotransporter cytotoxins among strains of enteroaggregative *Escherichia coli*. *Am J Trop Med Hyg* **2009**; 80:294–301.
- Jenkins C, van Ijperen C, Dudley EG, et al. Use of a microarray to assess the distribution of plasmid and chromosomal virulence genes in strains of enteroaggregative *Escherichia coli*. *FEMS Microbiol Lett* **2005**; 253:119–24.
- Nataro JP, Yikang D, Yingkang D, Walker K. AggR, a transcriptional activator of aggregative adherence fimbria I expression in enteroaggregative *Escherichia coli*. *J Bacteriol* **1994**; 176:4691–9.
- Bernier C, Gounon P, Le Bouguéne C. Identification of an aggregative adherence fimbria (AAF) type III-encoding operon in enteroaggregative *Escherichia coli* as a sensitive probe for detecting the AAF-encoding operon family. *Infect Immun* **2002**; 70:4302–11.
- Boisen N, Struve C, Scheutz F, Krogfelt KA, Nataro JP. New adhesin of enteroaggregative *Escherichia coli* related to the Afa/Dr/AAF family. *Infect Immun* **2008**; 76:3281–92.
- Czeczulin JR, Balepur S, Hicks S, et al. Aggregative adherence fimbria II, a second fimbrial antigen mediating aggregative adherence in enteroaggregative *Escherichia coli*. *Infect Immun* **1997**; 65:4135–45.
- Henderson IR, Hicks S, Navarro-García F, Elias WP, Phillips AD, Nataro JP. Involvement of the enteroaggregative *Escherichia coli* plasmid-encoded toxin in causing human intestinal damage. *Infect Immun* **1999**; 67:5338–44.
- Nataro JP, Yikang D, Giron JA, Savarino SJ, Kothary MH, Hall R. Aggregative adherence fimbria I expression in enteroaggregative *Escherichia coli* requires two unlinked plasmid regions. *Infect Immun* **1993**; 61:1126–31.
- Strauman MC, Harper JM, Harrington SM, Boll EJ, Nataro JP. Enteroaggregative *Escherichia coli* disrupts epithelial cell tight junctions. *Infect Immun* **2010**; 78:4958–64.
- Harrington SM, Strauman MC, Abe CM, Nataro JP. Aggregative adherence fimbriae contribute to the inflammatory response of epithelial cells infected with enteroaggregative *Escherichia coli*. *Cell Microbiol* **2005**; 7:1565–78.
- Dutta PR, Cappello R, Navarro-García F, Nataro JP. Functional comparison of serine protease autotransporters of enterobacteriaceae. *Infect Immun* **2002**; 70:7105–13.
- Frank C, Werber D, Cramer JP, et al. Epidemic profile of Shiga-toxin-producing *Escherichia coli* O104:H4 outbreak in Germany. *N Engl J Med* **2011**; 365:1771–80.
- Scheutz F, Nielsen EM, Frimodt-Møller J, et al. Characteristics of the enteroaggregative Shiga toxin/verotoxin-producing *Escherichia coli* O104:H4 strain causing the outbreak of haemolytic uraemic syndrome in Germany, May to June 2011. *Euro Surveill* **2011**; 16.
- Bielaszewska M, Mellmann A, Zhang W, et al. Characterisation of the *Escherichia coli* strain associated with an outbreak of haemolytic uraemic syndrome in Germany, 2011: a microbiological study. *Lancet Infect Dis* **2011**; 11:671–6.
- Rasko DA, Webster DR, Sahl JW, et al. Origins of the *E. coli* strain causing an outbreak of hemolytic-uremic syndrome in Germany. *N Engl J Med* **2011**; 365:709–17.
- Donnenberg MS, Kaper JB. Construction of an eae deletion mutant of enteropathogenic *Escherichia coli* by using a positive-selection suicide vector. *Infect Immun* **1991**; 59:4310–7.
- Sheikh J, Hicks S, Dall'Agnol M, Phillips AD, Nataro JP. Roles for Fis and YafK in biofilm formation by enteroaggregative *Escherichia coli*. *Mol Microbiol* **2001**; 41:983–97.
- Gentry MK, Dalrymple JM. Quantitative microtiter cytotoxicity assay for Shigella toxin. *J Clin Microbiol* **1980**; 12:361–6.
- Schmitt CK, McKee ML, O'Brien AD. Two copies of Shiga-like toxin II-related genes common in enterohemorrhagic *Escherichia coli* strains are responsible for the antigenic heterogeneity of the O157:H- strain E32511. *Infect Immun* **1991**; 59:1065–73.
- Hicks S, Candy D, Phillips A. Adhesion of enteroaggregative *Escherichia coli* to pediatric intestinal mucosa in vitro. *Infect Immun* **1996**; 64:4751–60.
- Zangari T, Melton-Celsa AR, Panda A, et al. Virulence of the Shiga toxin type 2-expressing *Escherichia coli* O104:H4 German outbreak isolate in two animal models. *Infect Immun* **2013**; 81:1562–74.
- Jiang Z-D, Greenberg D, Nataro JP, Steffen R, DuPont HL. Rate of occurrence and pathogenic effect of enteroaggregative *Escherichia coli* virulence factors in international travelers. *J Clin Microbiol* **2002**; 40:4185–90.
- Tran S-L, Billoud L, Lewis SB, Phillips AD, Schüller S. Shiga toxin production and translocation during microaerobic human colonic infection with Shiga toxin-producing *E. coli* O157:H7 and O104:H4. *Cell Microbiol* **2014**; 16:1255–66.
- Acheson DW, Moore R, De Breucker S, et al. Translocation of Shiga toxin across polarized intestinal cells in tissue culture. *Infect Immun* **1996**; 64:3294–300.

35. Hurley BP, Thorpe CM, Acheson DW. Shiga toxin translocation across intestinal epithelial cells is enhanced by neutrophil transmigration. *Infect Immun* **2001**; 69:6148–55.
36. Trachtman H, Austin C, Lewinski M, Stahl RAK. Renal and neurological involvement in typical Shiga toxin-associated HUS. *Nat Rev Nephrol* **2012**; 8:658–69.
37. Frankel G, Phillips AD. Attaching effacing *Escherichia coli* and paradigms of Tir-triggered actin polymerization: getting off the pedestal. *Cell Microbiol* **2008**; 10:549–56.
38. DeVinney R, Puente JL, Gauthier A, Goosney D, Finlay BB. Enterohaemorrhagic and enteropathogenic *Escherichia coli* use a different Tir-based mechanism for pedestal formation. *Mol Microbiol* **2001**; 41:1445–58.
39. Navarro-García F, Sears C, Eslava C, Cravioto A, Nataro JP. Cytoskeletal effects induced by pet, the serine protease enterotoxin of enteroaggregative *Escherichia coli*. *Infect Immun* **1999**; 67:2184–92.
40. Thorpe CM, Hurley BP, Lincicome LL, Jacewicz MS, Keusch GT, Acheson DW. Shiga toxins stimulate secretion of interleukin-8 from intestinal epithelial cells. *Infect Immun* **1999**; 67:5985–93.
41. Benjelloun-Touimi Z, Sansonetti PJ, Parsot C. SepA, the major extracellular protein of *Shigella flexneri*: autonomous secretion and involvement in tissue invasion. *Mol Microbiol* **1995**; 17:123–35.
42. Boll EJ, Struve C, Sander A, et al. The fimbriae of enteroaggregative *Escherichia coli* induce epithelial inflammation in vitro and in a human intestinal xenograft model. *J Infect Dis* **2012**; 206:714–22.
43. Hurley BP, Jacewicz M, Thorpe CM, et al. Shiga toxins 1 and 2 translocate differently across polarized intestinal epithelial cells. *Infect Immun* **1999**; 67:6670–7.
44. Zhang W, Bielaszewska M, Kunsmann L, et al. Lability of the pAA Virulence Plasmid in *Escherichia coli* O104:H4: Implications for Virulence in Humans. *PLoS One* **2013**; 8:e66717.
45. Munera D, Ritchie JM, Hatzios SK, et al. Autotransporters but not pAA are critical for rabbit colonization by Shiga toxin-producing *Escherichia coli* O104:H4. *Nat Commun* **2014**; 5:3080.
46. Griffin PM, Ostroff SM, Tauxe RV, et al. Illnesses associated with *Escherichia coli* O157:H7 infections. A broad clinical spectrum. *Ann Intern Med* **1988**; 109:705–12.
47. Simons RW, Houman F, Kleckner N. Improved single and multicopy lac-based cloning vectors for protein and operon fusions. *Gene* **1987**; 53:85–96.
48. Levine MM, Bergquist EJ, Nalin DR, Waterman DH, Hornick RB, Young CR SS. *Escherichia coli* strains that cause diarrhoea but do not produce heat-labile or heat-stable enterotoxins and are non-invasive. *Lancet* **1978**; 311:1119–22.
49. Guzman LM, Belin D, Carson MJ, Beckwith J. Tight regulation, modulation, and high-level expression by vectors containing the arabinose PBAD promoter. *J Bacteriol* **1995**; 177:4121–30.
50. Harrison LM, Rallabhandi P, Michalski J, et al. *Vibrio cholerae* flagellins induce toll-like receptor 5-mediated interleukin-8 production through mitogen-activated protein kinase and NF-kappaB activation. *Infect Immun* **2008**; 76:5524–34.